Available online at www.sciencedirect.com
SCIENCE DIRECT®
Analytica Chimica Acta 495 (2003) 177–193
ANALYTICA CHIMICA ACTA
www.elsevier.com/locate/aca

Exploratory analysis of L'vov platform surfaces for electrothermal atomic absorption spectrometry by using three-way chemometric tools

Edenir R. Pereira-Filho, Marcelo M. Sena, Marco A.Z. Arruda, Ronei J. Poppi*

Depto. de Química Analítica, Instituto de Química, Universidade Estadual de Campinas—UNICAMP, P.O. Box 6154, CEP 13083-862, Campinas, SP, Brazil

Received 18 December 2002; received in revised form 24 June 2003; accepted 7 August 2003

Abstract

An exploratory analysis of the effects of permanent (Zr) and conventional (Mg and a mixture of Pd+Mg) chemical modifiers on L'vov platforms for electrothermal atomic absorption spectrometry (ETAAS) was performed in this work by using two chemometric tools. Twelve L'vov platforms were used for Al, Cd and Pb determination in biological slurry samples. For each platform, a different combination of chemical modifier, number of heating cycles and determined analyte was employed. The morphology of the platforms was evaluated using scanning electron microscopy (SEM) and the obtained data was analysed with image principal component analysis (image PCA). The results allowed differentiating the platform treated with Mg from the other platforms. In addition, eight residual species (P, S, Ca, Ti, Fe, Zr, Hf and Pd) distributions were obtained by using micro synchrotron radiation X-ray fluorescence (μSRXRF) in the same platforms for 100 points across the horizontal axis. These data were modelled with orthogonal constrained PARAllel FACtor analysis (PARAFAC) and a global characterisation of the platforms was achieved. Four platforms presented a particularly behaviour, being so different among themselves, that it was necessary one specific factor (1–4) to model each one. Factor 5 demonstrated that two platforms presented a similar behaviour characterised by high Ca and, to a lesser extent, Ti content. Finally, factor 6 modelled the correlated behaviour of five platforms characterised by Zr content. It was also observed that the platform morphology has a good connection with the residual species found in its surface. This kind of study can open a vast field to exploratory analysis of L'vov platforms in ETAAS.

Keywords: L'vov platforms; ETAAS; μSRXRF; PARAFAC; Image PCA; Permanent and conventional chemical modifiers

1. Introduction

Nowadays, the amount and the complexity of information in analytical chemistry are increasing due to the development of new and faster techniques. Among these techniques, those related to atomic absorption spectrometry have received special attention. In electrothermal atomic absorption spectrometry (ETAAS) with graphite tube atomiser, there has been a considerable development in devices and processes, such as ultrasound probe [1], background corrector based on Zeeman-effect with transversal heated graphite atomiser (THGA) [2] and stabilised temperature platform furnace (STPF) [3]. The combination of these tendencies with permanent chemical modifiers and slurry analysis has been subject to a great number of

* Corresponding author. Tel.: +55-19-37883126; fax: +55-19-37883023.
E-mail address: ronei@iqm.unicamp.br (R.J. Poppi).

0003-2670/$ – see front matter © 2003 Elsevier B.V. All rights reserved.
doi:10.1016/j.aca.2003.08.015

investigations in the recent literature. The applications can be found in a large way from simple biological [4] to more complex sediment samples [5]. In addition, the use of slurry samples shows the advantage of a simpler pre-treatment process with less time consumption and reduction or elimination of contamination problems [6]. Nevertheless, few contributions have been made related to graphite surface interactions with permanent modifiers and atomisation mechanisms using the conditions described in the present work [7].

It is important to note that such kind of studies can lead to a better understanding of problems related to atomisation mechanisms. However, it is not an easy task to shed light on this kind of matter, as mentioned by Volynsky [8], who has investigated the mechanisms of the action of chemical modifiers for ETAAS. He has emphasised the difficulties and limitations that analytical chemists have faced when proposing these mechanisms and the ineffectiveness of some of the published previous studies to propose suitable mechanisms when chemical modifiers are applied. Taking these considerations into account, a better understanding of the effects of chemical modifiers on ETAAS must combine this technique with other types of analytical and image techniques. These analytical and/or image techniques should provide in situ analysis of the platform surface, such as scanning tunnelling microscopy (STM) [9], scanning electron microscopy (SEM) [10], laser desorption mass spectrometry and differential scanning calorimetry [11], X-ray photoelectron spectroscopy (XPS) [12] and micro synchrotron radiation X-ray fluorescence (μSRXRF) [13]. The μSRXRF, used in this work, is particularly a versatile non-destructive technique that allows the analysis of non-conducting samples without coating or vacuum requirements and avoids sample preparation.

On the other hand, this combination of analytical techniques generates a large amount of data and it is almost impossible to handle them only by observing graphics or images. In such a case, it is necessary to use more powerful and accurate tools to extract information from the data. Chemometric methods have widely been used for exploratory investigation of analytical data and the most common is the principal component analysis (PCA) [14]. PCA projects the high dimensional data onto lower dimensional space. This procedure permits to get a few linear combinations of the original variables (principal components, PCs) and allows the interpretation of better-summarised information. Notwithstanding, the increasing complexity of analytical data has limited the use of the PCA in several situations.

In the last decade, a three-way (or three-mode) analysis was introduced in the field of chemometrics [15]. A three-way array may be obtained by collecting data tables with a fixed set of objects and variables under different experimental conditions such as sampling time, temperature, pH, etc. The tables collected under various conditions can be stacked providing a three-dimensional arrangement of data. The most common type of data analysed by these methods has been that generated by hyphenated methods, such as fluorescence spectroscopy [16,17] and high-performance liquid chromatography with diode array detection (HPLC-DAD) [18]. Other types of three-way data suitable for chemometric analysis can be found in QSAR modelling [19], process control [20], kinetic [18] and environmental [21] analysis. The main three-way methods are PARAllel FACtor analysis (PARAFAC) [22,23], Tucker3 [24] and N-PLS [25]. Three-way data can also be unfolded to a two-way matrix and treated with the PCA [23]. This strategy is usually employed in multivariate image analysis [26,27], in whose context it is namely image PCA.

The exploratory analysis is not actually a model, but a process, where each proposed model gives new insight and knowledge of the physicochemical phenomena that generate the data. The main purpose of an exploratory analysis is to learn from the data the interrelationship between variables and objects with a minimum of a priori assumptions. However, the purpose of modelling data with PARAFAC has mainly been to solve problems related to curve resolution and calibration [22,23]. In fact, PARAFAC has been used for exploratory analysis [28] to a lesser extent. Besides, in spite of its increasing application in analytical chemistry, its use in atomic spectrometry is not common. In this sense, only two articles have applied PARAFAC for atomic spectrometry data: Marcos et al. [29] have investigated long-term stability in ICP-OES and Moreda-Piñeiro et al. [30] have studied systematic error in ICP-OES and mass spectrometry.

According to what was discussed above, the aim of this work was to perform an exploratory analysis of the effects of different chemical modifiers (permanent and conventional) on L'vov platforms for ETAAS with

the aid of two chemometric tools. It was the purpose of this work to correlate the visual information obtained with micrographs and surface distributions of remain species after atomisation processes. This information was obtained from 12 L'vov platforms treated with a permanent chemical modifier, Zr, or conventional modifiers, such as Mg and a mixture of Pd and Mg. These platforms were used for Al, Cd and Pb determination in biological slurry samples. The visual information was obtained as micrographs using SEM and treated with image PCA. Species distribution on platforms surface was obtained with μSRXRF and a global characterisation of the effects of modifiers or concomitants was possible by using PARAFAC in combination with image PCA.

2. Theory

2.1. Multivariate image analysis and unfolded-PCA

A multivariate image is a three-way array of data, with two of the ways being geometrical image coordinates (pixels coordinates) and one a "variable", allowing the use of PCA for data interpretation in variable space. In contrast to the analysis of a two-way data matrix, the majority of the results can be shown visually. It must be understood that two of the ways are essentially different from the third one and they are usually treated as a pair, because the horizontal and vertical image dimensions work together to describe the image plane. The variable way is much more different from the other two, since it can represent wavelength, electron energy, mass, chemical modifier on platform for ETAAS (our case), etc. [26,27].

In situations where the variable space is emphasised, it may be useful to ignore temporarily the geometry of the image. Then, the three-way array $\underline{\boldsymbol{X}}$ of dimensions I, J and K can be reorganised (unfolded) into a long matrix $\boldsymbol{X}$ of size $I \times J \times K$ and this new matrix treated with a two-way PCA. Notice that the image pixels are treated as objects, which vary with the third dimension. This is the image PCA. The data array $\underline{\boldsymbol{X}}$ is decomposed into a sum of pixel image score matrices $\boldsymbol{T}_a$ and variable loading vectors $\boldsymbol{p}_a$ according to the following formula (1), where $\underline{\boldsymbol{E}}$ is a matrix of residuals, $a = 1$ to A the number of principal components and the symbol $*$ means the Kronecker product [23]

$$\underline{\boldsymbol{X}} = \sum_{a=1}^{A} \boldsymbol{T}_a * \boldsymbol{p}_a + \underline{\boldsymbol{E}} \tag{1}$$

So, loading plots are useful for carrying out exploratory analysis or classification of the entities under study, as exemplified by Pereira-Filho et al. [31]. Finally, it is important to note that image PCA is not a proper three-way method, because it uses a two-way decomposition for three-way data.

2.2. PARAFAC

PARAllel FACtor analysis is a decomposition method for three-way data, which was first developed by psychometricians in the early 1970s. The decomposition is made into triads or trilinear factors. Instead of one score vector and one loading vector, as in bilinear PCA, each factor consists of three loading vectors. It is not usual to distinguish between scores and loadings since they are treated numerically as equals. Another important difference between PCA and PARAFAC is that in PARAFAC there is no need of requiring orthogonality to identify the model. As a consequence, non-orthogonal PARAFAC models are not nested, i.e. the parameters of an $F+1$ factor model are not equal to the parameters of an F factor model plus one additional factor. PARAFAC can also be considered a constrained version of the more general Tucker3 method [24] with a superidentity core matrix. It is less flexible, uses fewer degrees of freedom and provides a unique solution that is not dependent on rotation. This last feature, known as uniqueness, turns PARAFAC very suitable for some kind of data, such as those originated from hyphenated methods [22].

Three loading matrices, A, B and C, with elements a_{if}, b_{jf} and c_{kf}, give the structural model behind PARAFAC. The model is adjusted to minimise the sum of squares of the residuals e_{ijk} in the following Eq. (2):

$$X_{ijk} = \sum_{f=1}^{F} a_{if} b_{jf} c_{kf} + e_{ijk} \tag{2}$$

where $f = 1$ to F is the number of factors. Finally, another important aspect to mention is the use of constraints aiming at improving the interpretability or the

stability of the PARAFAC model. The fitness of a constrained model will always be lower than the fitness of an unconstrained model, but if the constrained one is more interpretable and realistic, these facts justify the decrease in fitness. The most used constraints are non-negativity, orthogonality and unimodality [23].

3. Experimental

3.1. Apparatus

A Perkin-Elmer Analyst 600 atomic absorption spectrometer (Überlingen, Germany) was employed using a longitudinal Zeeman-effect background correction system, as well as graphite atomiser tubes with integrated L'vov platforms. All measurements were based on integrated absorbance and performed at 309.3, 228.8 and 283.3 nm for Al, Cd and Pb, respectively. A hollow cathode lamp was used as primary radiation source for Al determination, and electrodeless discharge lamps (EDL) were used for Cd and Pb determinations. The electron micrographs were obtained by employing a Jeol model JSM-T300 electron-scanning microscope (Tokyo, Japan). A TCE S440 scanner was used for images digitalisation. The experiments using μSRXRF were made at the Brazilian National Laboratory of Synchrotron Light (LNLS, Campinas, Brazil) [32,33].

3.2. Reagents, solutions and slurry samples

Deionised water was used throughout the experiments. Al and Pb standard stock solutions (1000 $mg\,l^{-1}$) were prepared from $Al(NO_3)_3{\cdot}9H_2O$ and $Pb(NO_3)_2$ (Ecibra, São Paulo, Brazil), respectively. A 1000 $mg\,l^{-1}$ Cd standard stock solution was prepared from $CdCl_2{\cdot}H_2O$ (Merck, Darmstadt, Germany). A 1 $g\,l^{-1}$ Zr solution was prepared from $ZrO(NO_3)_2$ (Acros, USA). The Mg conventional modifier [0.003 mg of $Mg(NO_3)_2$] was prepared from $Mg(NO_3)_2{\cdot}6H_2O$ (Merck) and the mixture of Pd and Mg used as a conventional modifier [0.005 mg of Pd + 0.003 mg of $Mg(NO_3)_2$] were prepared from $Mg(NO_3)_2{\cdot}6H_2O$ and $Pd(NO_3)_2$ (Aldrich, Milwaukee, USA). In the determination procedure, 10 μl of Mg or Pd + Mg as a conventional modifier was introduced together with a slurry sample into the L'vov platform. The solutions of these conventional modifiers were prepared according to the user's manual [34].

A commercial milk powder was used for preparing the slurry samples for Al determination. The slurry was prepared by weighting 1000 mg of milk powder (particle size 75–150 μm) in a 100 ml volumetric flask. Certified samples were used for Cd and Pb determinations. Slurries were prepared with a bovine liver (SRM 1577b) sample (100 mg in 25 ml) and a beech leaves (CRM 100) sample (40 mg in 10 ml) for Cd and Pb, respectively. Nitric acid 0.2% (v/v) (Merck) was used to complete the volumes. An ultrasound bath (Branson, 5200, Danbury, USA) was used for previous slurries homogenisation and stabilisation.

3.3. Platforms and chemical modifiers

Twelve different platforms were studied in this work. Two platforms (numbers 1 and 2) were analysed without any previous use. One of them was analysed brand new, without any chemical modification. The other new platform was treated with 500 μg of Zr following the heating program procedure described in a previous work [7]. In this procedure, 50 μl of 1 $g\,l^{-1}$ Zr solution were collected using the auto-sampler pipette and delivered into the L'vov platform and then a heating program was performed. This procedure was repeated 10 times.

Other five platforms (numbers 3–7) were treated with Zr and were used for Al determination in a commercial milk powder prepared as slurry sample. These platforms were used for 50, 100, 150, 200 and 500 heating cycles, and the Zr treatment was repeated after 50 determinations. This procedure was adopted because the temperatures for Al pyrolysis (1100 °C) and atomisation (2400 °C) are very high. The heating program for Al determination can be seen in Table 1.

Aiming at comparing the Zr performance as a permanent chemical modifier for Al determination, a platform (8) treated conventionally with Mg was used for 500 heating cycles. Two platforms (9 and 10) were treated only one time with 500 μg of Zr and were utilised for Cd and Pb determination in bovine liver and beech leaves slurries, respectively. Cd and Pb were determined for 1100 and 864 heating cycles, respectively. The performance of two another platforms (11 and 12), treated conventionally with a mixture of Pd

Table 1
Heating programs employed for Al, Cd and Pb determination

Step	Temperature (°C)	Ramp (s)	Hold (s)	Ar flow rate (ml min^{-1})
1	110	5	25	250
2	130	15	30	250
3	[a]	10	20	250
4	[b]	0	[c]	0
5	[d]	1	3	250

[a] Pyrolysis temperatures of 1100, 400 and 700 °C for Al, Cd and Pb, respectively.
[b] Atomisation temperatures of 2400, 1900 and 2000 for Al, Cd and Pb, respectively.
[c] Hold time of 3 s for Al and Cd and 4 s for Pb.
[d] Clean temperature of 2450 for Al and 2200 °C for Cd and Pb.

and Mg as chemical modifier, was also checked for Cd and Pb determinations. In this case, the numbers of heating cycles were 200 and 416, respectively. The heating programs used for Cd and Pb determination are also shown in Table 1.

For Cd and Pb determination, the platforms were treated only once at the beginning of the experiments with Zr. The criterion for stopping the analysis was applied after carefully watching the integrated absorbance of 2 and 50 μg l^{-1} standard solution, respectively. This criterion was established when the difference observed between the first and the last results was more than 20%. In some cases, this observation was not used because several platforms were broken due to the high frequency of heating cycles.

The use of conventional chemical modifiers (Mg and Pd + Mg) was made as in a previous work [7], and the heating programs were the same used when Zr was employed as permanent modifier (Table 1). In order to get a better comprehension, a summary of the studied L'vov platforms is shown in Table 2.

3.4. Scanning electron microscopy and μSRXRF analysis

After metals determinations the morphology of each platform was visualised by using a scanning electron microscope. Ten images were sequentially acquired across the horizontal axis from each platform. The magnification was 500 times, the accelerating voltage was 20 kV and the distance between each consecutive micrograph was around 1 mm, covering the whole platform extension (around 10 mm).

During the experiments with μSRXRF, a white beam light of 30 μm in diameter was used. Each platform was mapped during 2 h. Signals from 113 points on the platform surface were collected. The first 13 points were rejected because during the data acquisition a contribution from the sample holder was observed at the first points of the scanning process. Each point was analysed during 60 s and the evaluated distance between two consecutive points was approximately 62 μm. The measurements started from the fixation point of the L'vov platform in the THGA tube to approximately 7 mm in the same direction. This procedure performed a scanning across the horizontal

Table 2
Summary of experiments carried out with L'vov platforms

Platform number	Analyte	Modifier[a] (number of treatments)	Number of heating cycles	Slurry sample
1	–	–	–	–
2	–	Zr (1)	–	–
3	Al	Zr (1)	50	Milk powder
4	Al	Zr (2)	100	Milk powder
5	Al	Zr (3)	150	Milk powder
6	Al	Zr (4)	200	Milk powder
7	Al	Zr (10)	500	Milk powder
8	Al	Mg (500)	500	Milk powder
9	Cd	Pd + Mg (200)	200	Bovine liver
10	Cd	Zr (1)	1100	Bovine liver
11	Pb	Zr (1)	864	Beech leaves
12	Pb	Pd + Mg (416)	416	Beech leaves

[a] Zr was used as permanent chemical modifier. Mg and the mixture of Pd + Mg were used as conventional modifiers.

axis (in the same way as for micrographs acquisition). The used 100 points were from 812.5 to 7000 μm across the horizontal axis of the platforms. During the scanning process, neither vacuum requirement nor platform treatment with a conductive material were necessary. The system set-up used in the platforms scanning was the same employed in a previous work [7]. After scanning experiments a total of eight species were found: Ca, Fe, Hf, P, Pd, S, Ti and Zr.

3.5. Data handling

3.5.1. Multivariate image analysis

The data were handled using MATLAB software, version 6.1 (The MathWorks, Natick, USA). The image PCA routine comes from the "PLS Toolbox", version 2.0 (Eigenvector Technologies, Manson, USA). After micrographs acquisition was finished, the images were digitalized using Photo Suite software. Then the images were converted into bitmap files and read using MATLAB. Finally, 120 matrices were obtained, i.e. 10 images from each platform, each one with 425 rows by 650 columns. The resolution used was 8 bits, which corresponds to 256 tonalities varying from black to white. Using multivariate image analysis, the images were transformed into numerical information, which can be treated as analytical data. In order to use image PCA, 120 matrices were arranged in a three-dimensional array of 650 columns × 425 rows × 120 variables. No image pre-processing was performed.

3.5.2. PARAFAC

The data were handled using MATLAB. PARAFAC modelling was carried out using "The *N*-way Toolbox for MATLAB", version 2.00 (R. Bro, Foodtechnology, Kopenhagen, Denmark) [35]. A $12 \times 8 \times 100$ three-way array was built: 12 different L'vov platforms, 8 remain species signals obtained using μSRXRF after atomisation processes and 100 points collected across the horizontal axis for each platform surface and for each remain species. The data pre-processing used was scaling within the second mode to unit square variation, in order to give equal weights to each variable/remain species distribution in the model. Scaling three-way data should take the trilinear model into account [22,23,36] and therefore, whole matrices instead of rows must be scaled. Direct trilinear decomposition was used for initialisation.

It was used the core consistency diagnostic (CORCONDIA) as a tool for model validation. CORCONDIA has been suggested for determining the proper number of factors for three-way models [23,37]. As PARAFAC can be considered a special case of Tucker3 [24] with a superidentity core matrix, the core consistency is based on the calculation of a $\underline{\boldsymbol{G}}$ Tucker3 core matrix from the PARAFAC factor matrices. If $\underline{\boldsymbol{G}}$ matrix has all the superdiagonal elements close to one and the off-superdiagonal elements close to zero, the PARAFAC model is not overfitted and the core consistency is close to 100%. Hence, a core consistency above 90% can be considered as indicative of an appropriate model, whereas a value in the neighbourhood of 50% indicates a problematic model with some lack of trilinearity. A core consistency close to zero or negative means an invalid PARAFAC model, which is not describing trilinear variation in the data. An invalid core consistency indicates that too many factors have been extracted, the model is either miss-specified or gross outliers are disturbing it. The core consistency decreases slightly with the increase in the number of factors, but very sharply when the correct number is exceeded. Therefore, the chosen model should have the highest number of factors and a valid core consistency.

A final remark is the use of constraints. Orthogonality constraints [22,23] can help to avoid problems with degeneracy, thus stabilising the solution. In this work, we imposed orthogonality constraint in the first mode aiming at extracting more factors. Orthogonality constraints are rarely used to chemometrics approaches, because they are not adequate for the most common applications in curve resolution. However, they can be useful for more exploratory purposes, as they permit variance partitioning of the otherwise correlated factors, allowing a more straightforward interpretation of the data. It is important to note that in this case, as in PCA, the solution of the PARAFAC model is nested.

4. Results and discussion

4.1. μSRXRF analysis

The platforms of Table 2 were analysed employing μSRXRF. In these experiments, 113 points were

scanned across the horizontal platform axis (the same procedure used in micrographs acquisition). After scanning experiments, a total of eight species were found. Zirconium was found in all platforms, which were treated permanently with this metal. In addition, Hf and Ti were also found in the platforms treated with Zr and used for more than 500 heating cycles. The Zr, Hf and Ti fluorescence intensities follow the same distribution on the platform heated by 500 cycles and used for Al determination, as observed in the previous work [7]. On the other hand, the distribution of these metals on the platforms treated with Zr and used for Cd and Pb determination (platforms 10 and 11) does not show the same trend. The presence of Hf and Ti together with Zr can be explained as impurities presented in the Zr salt. However, these metals did not offer any problems for Al, Cd and Pb determinations, since they have also been used as permanent chemical modifiers [38,39].

Palladium was found mainly in the platforms treated with a mixture of Pd and Mg (platforms 9 and 12). High calcium fluorescence intensity was detected mainly in the platforms treated with conventional modifiers (Mg and Pd + Mg). This fact can prove that the conventional modifiers were not successful in the concomitant elimination. It was verified that the platforms treated with conventional modifiers presented more residual species (for example Cd determination using Pd + Mg (platform number 9)) than the platforms treated with Zr. On the other hand, platforms used for Cd determination (400 and 1900 °C for pyrolysis and atomisation, respectively) presented more residual species than the other platforms. Platforms used for Cd and Pb determination did not present fluorescence intensity for these metals, confirming that the heating programs (Table 1) used were efficient for analytes determinations.

4.2. Scanning electron microscopy and multivariate image analysis

Ten equally spaced micrographs were sequentially obtained across the horizontal platforms axes in the scanning electron microscopy. This procedure was adopted to obtain a more in-depth platform morphology characterisation. After micrographs acquisition, 120 images were obtained from the 12 platforms already described in Table 2.

After multivariate image analysis, it was obtained a model with PC1 accounting for 63.4% of the variance and the remaining information distributed in very small contributions from tens of components. This type of behaviour is typically observed in image PCA [7,27,31]. Each following PC's accounted for only 0.4% or less of the variance and did not represent any clearly interpretable trend. The loading plot of PC1 is showed in Fig. 1. The image loadings were presented from the beginning (fixation point) to the end for each platform. The new platforms (1 and 2), the more preserved ones, showed high loading values on PC1. The platforms treated with Zr and used for Al determination for 50–150 heating cycles (3–5) presented, mainly in the edges, a similar behaviour, indicating that their surfaces were almost so preserved as the new platforms. The platforms treated with Zr and used for Al determination for 200 and 500 heating cycles (6 and 7) showed lower values on PC1, probably due to more abraded surfaces. The platform treated with Zr and used for Cd determination (10) presented, even heated for 1100 heating cycles, PC1 values similar to the new platforms. The platforms treated with Pd and Mg (9 and 12) presented surfaces different from the new ones. It is interesting to point out that these platforms were used for only 200 and 416 heating cycles.

The most remarkable trend observed in Fig. 1 was related to platform 8, used for Al determination and treated with Mg. Micrographs obtained from the platform centre presented the smallest values for PC1, leading to the conclusion that this platform has the most abraded surface. In this case, the modification with Mg was not so effective as Zr for the platform surface preservation. It is important to point out that these observed differences were not clear only by observing the images. In this case, after image PCA analysis it was found some evidences that probably the chemical modification was responsible for this separation. A more in-depth investigation can be a correlation between the visual information and the residual species observed.

4.3. PARAFAC

An univariate analyses of this data could be performed, but in this case, due to the number of platforms (12), remained species (8) and scanned positions (100), a great number of graphics (at least 96)

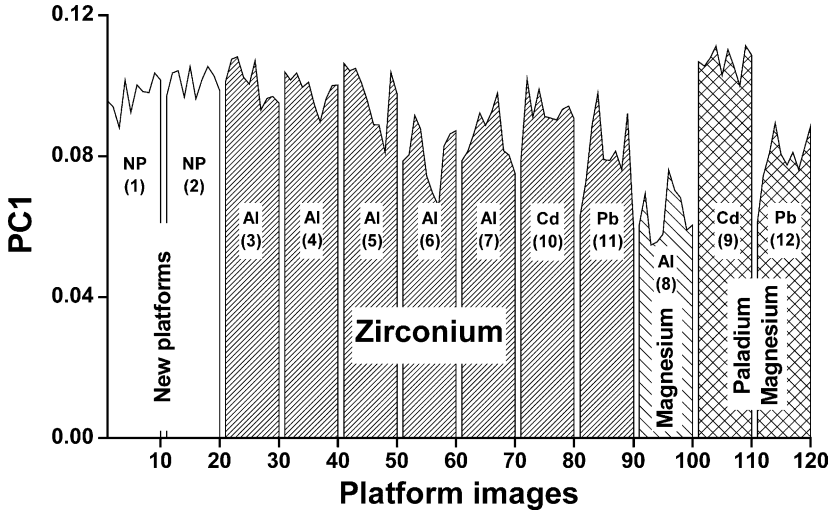

Fig. 1. Loading plot of PC1 (63.4%) obtained in image PCA for 120 micrographs. The micrographs for each platform are sequentially presented from the beginning to the end, and the numbers in parenthesis represents the platform order (Table 2).

has to be generated and some information about, for example, a specific platform position, could be lost or not detected by the analyst. In this way, to summarise and better visualise the results obtained by the μSRXRF analysis, it was tried to use a multivariate chemometric tool to aid data analysis.

According to the results obtained when the image PCA was applied, it is expected to get a relation between the images from a specific platform and its residual species distributions obtained with μSRXRF.

In this context, it was firstly tried to apply bi-dimensional PCA to an unfolded array of scanning remain species distributions. A matrix composed by 96 samples (12 platforms × 8 species) and 100 variables (scanning positions) was analysed. The data were autoscaled prior to analysis and a scatter plot of PC1 × PC2 (not shown) only clearly separate two points from the rest, platform 9/Ti (content of Ti on platform 9) and platform 12/Pd. After withdrawing these two points, another PCA analysis was carried out and the result showed that PC2 separated platform 10/Ti from the rest while the other points were distributed along PC1 axis. However, it was not possible to characterise the platforms treated with Zr and Mg (the most abraded platform according to image PCA) and used for Al determination (3–8). Also, a joint interpretation of loading and scores was not leading to any clearly conclusion. The limitations of the results obtained by unfolding PCA can be understood by a comparison with true multi-way models, such as PARAFAC. Unfolding PCA ignores the multi-way structure of the data, while PARAFAC model imposes more structure to the data and hence, filters away more variation/noise, leading to a more robust, more interpretable and parsimonious model [23].

An array composed by 12 platforms × 8 species × 100 scanning points was modelled by PARAFAC. The assumption is that our data may present a trilinear behaviour and the PARAFAC modelling allows to better platforms characterisation as a function of their previous chemical modifications. Without any constraint imposed to the data, a four-factor was considered the best model with a core consistency of 99.9% and accounting for 71.1% of the total variance. A five-factor model was considered inappropriate because it presented a negative core consistency (−1.9%). Since we observed that some trends in data were out of the model (mainly Ca and Ti and some platforms presented high values in the residues), we decided to impose orthogonality constraint on the first mode, aiming at modelling more variance and evidencing the differences among platforms. As a consequence, the obtained factors corresponding to the platforms were forced to be non-correlated. Then, a six-factor constrained model was considered the best with a core consistency of 95.0% and accounting

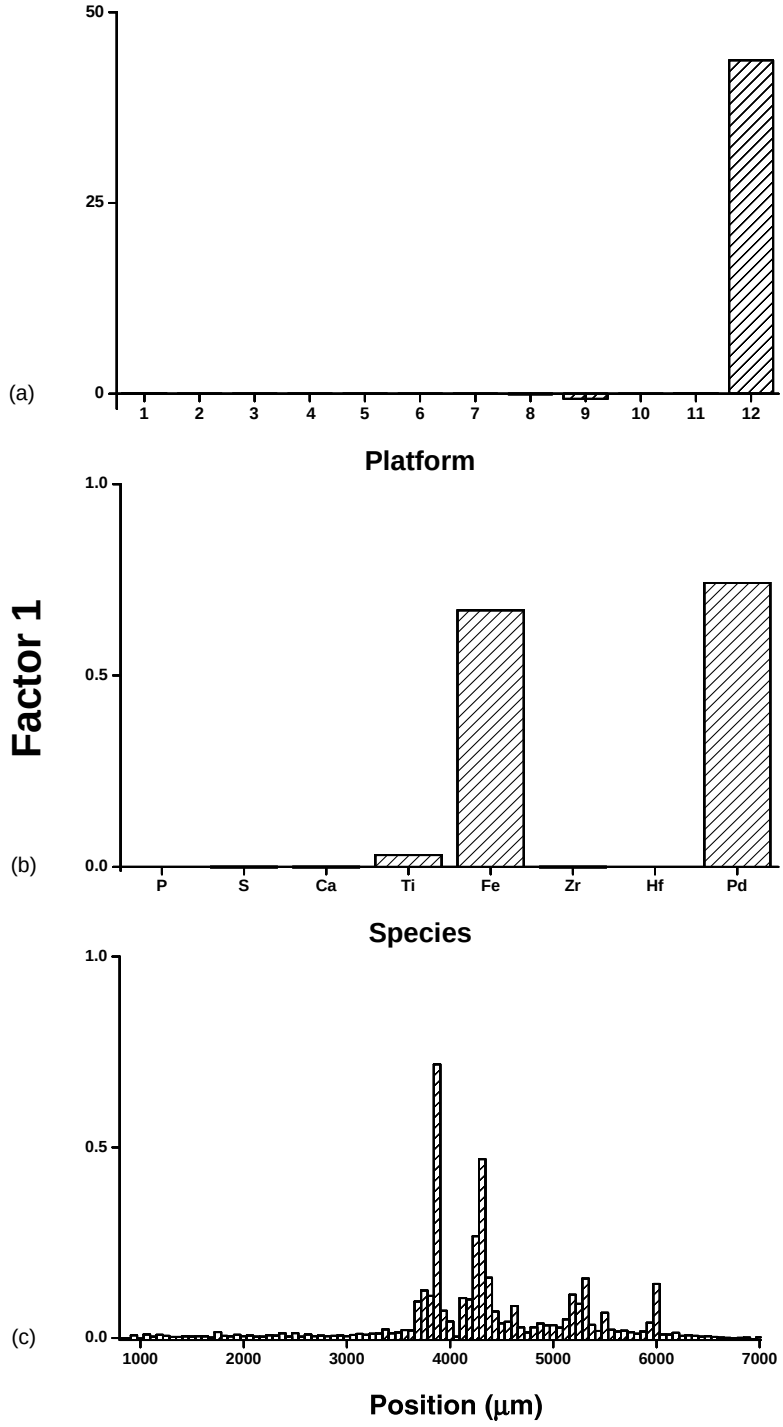

Fig. 2. PARAFAC results for factor 1: (a) platform mode; (b) species mode; and (c) position mode loadings.

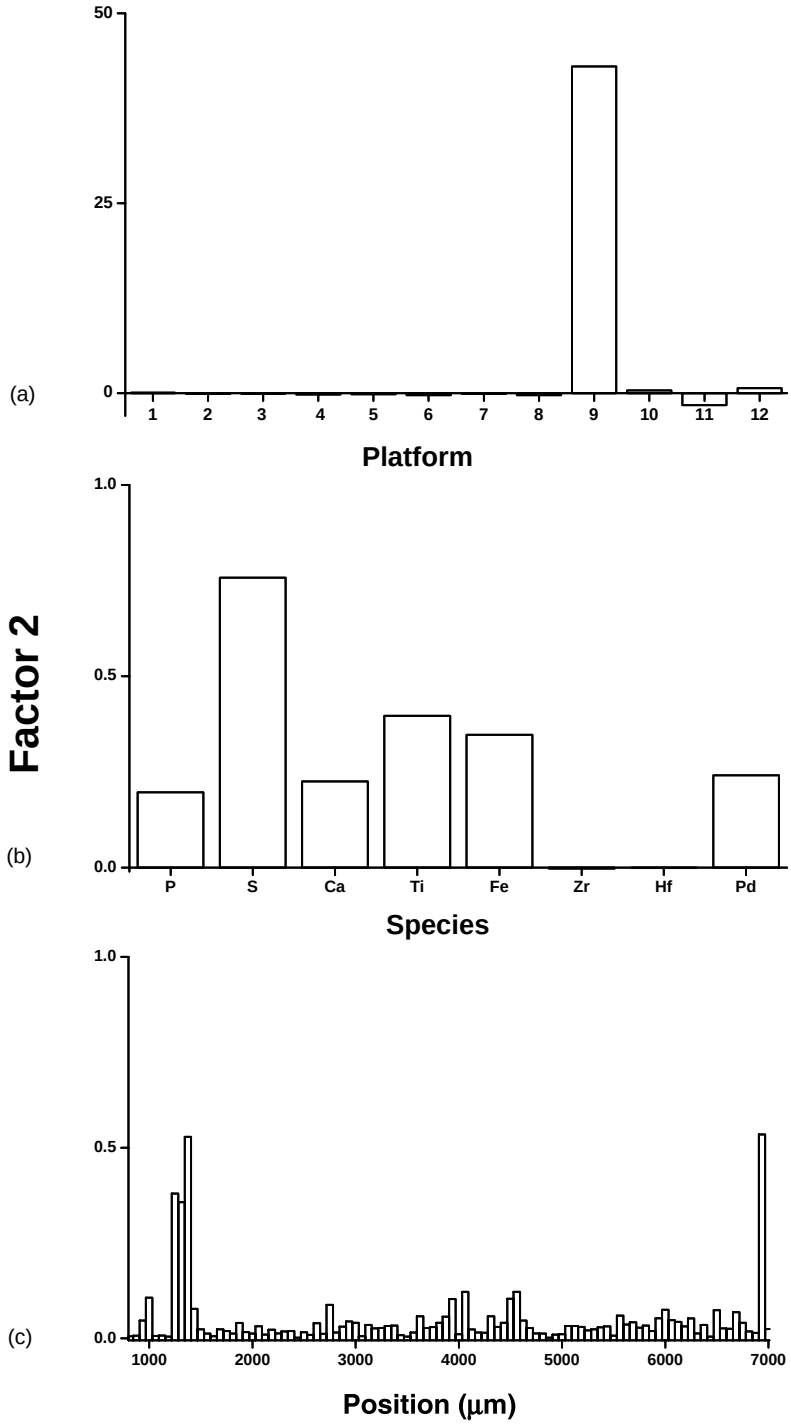

Fig. 3. PARAFAC results for factor 2: (a) platform mode; (b) species mode; and (c) position mode loadings.

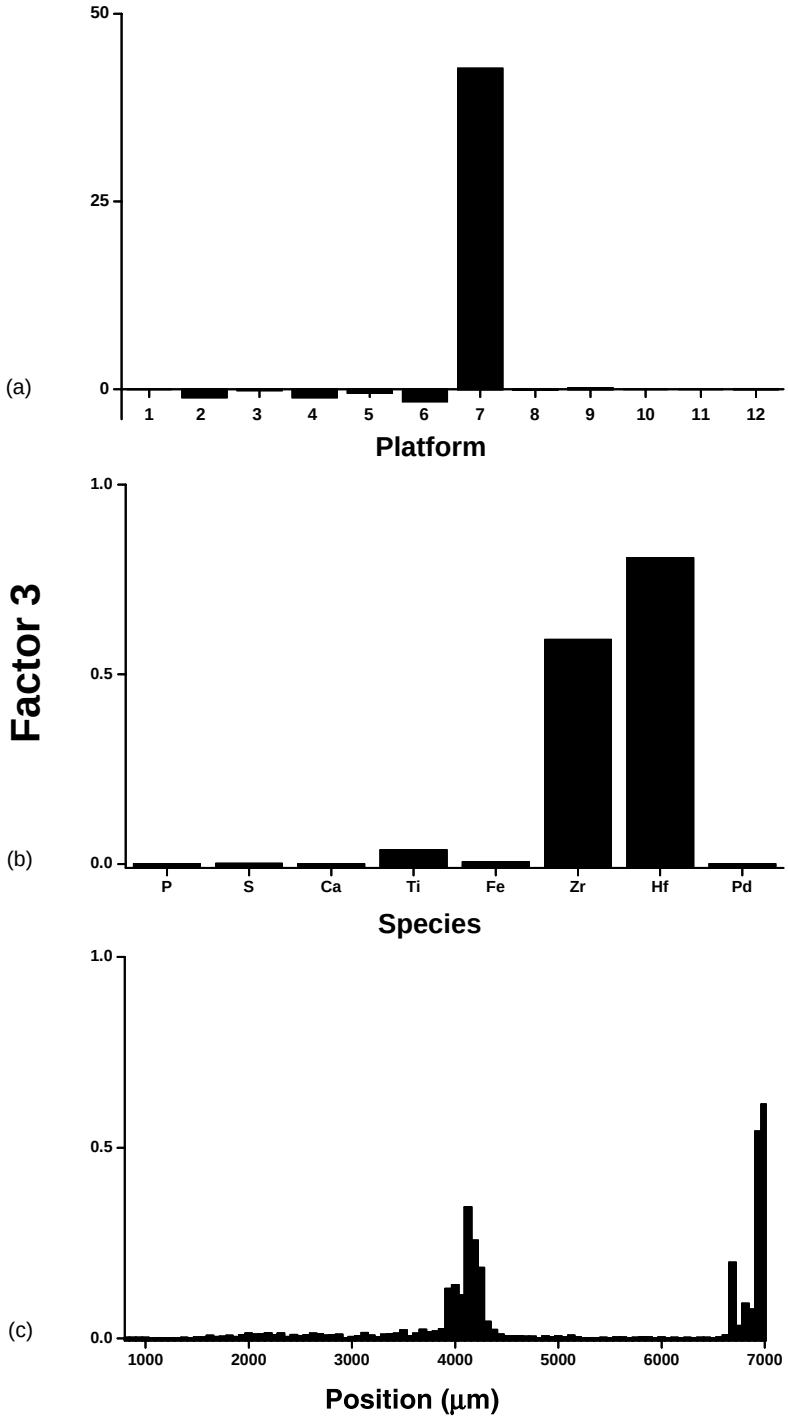

Fig. 4. PARAFAC results for factor 3: (a) platform mode; (b) species mode; and (c) position mode loadings.

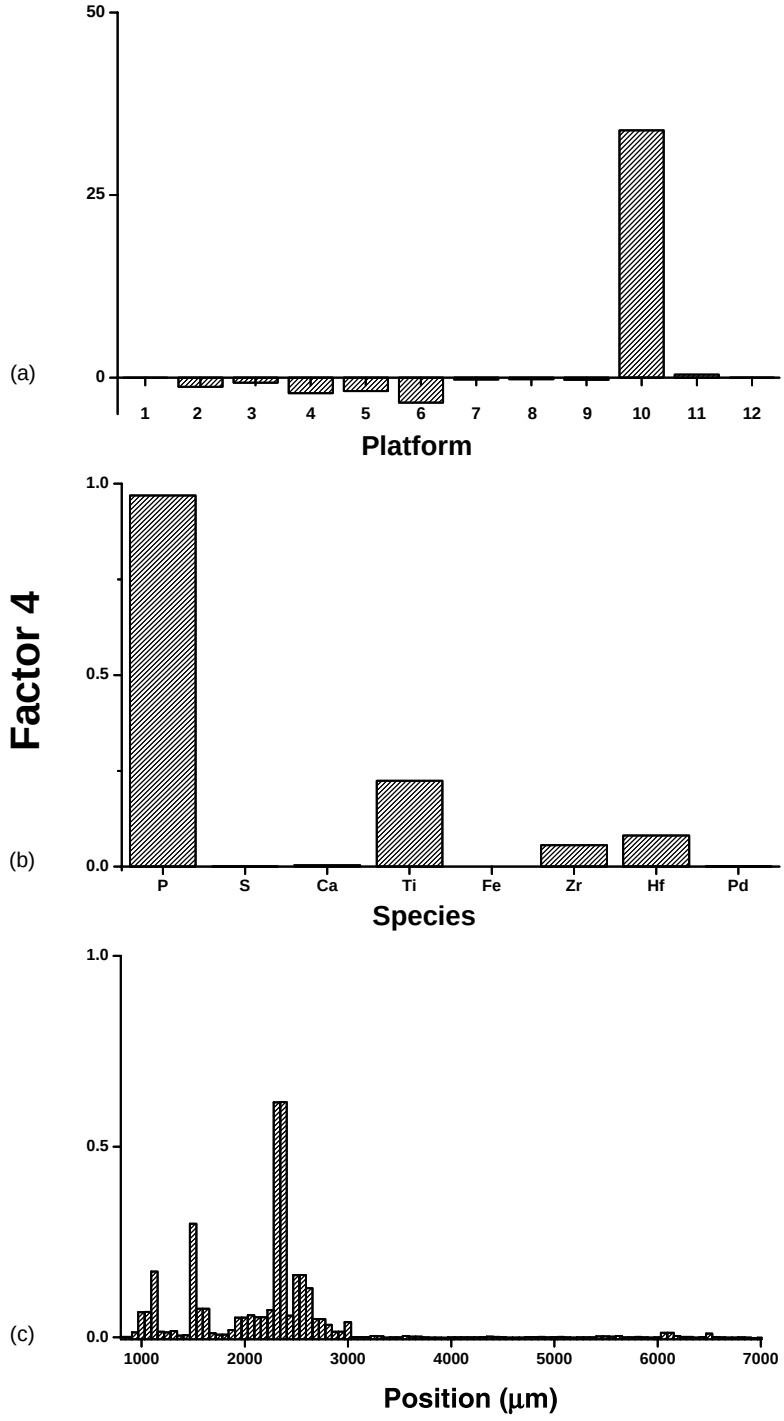

Fig. 5. PARAFAC results for factor 4: (a) platform mode; (b) species mode; and (c) position mode loadings.

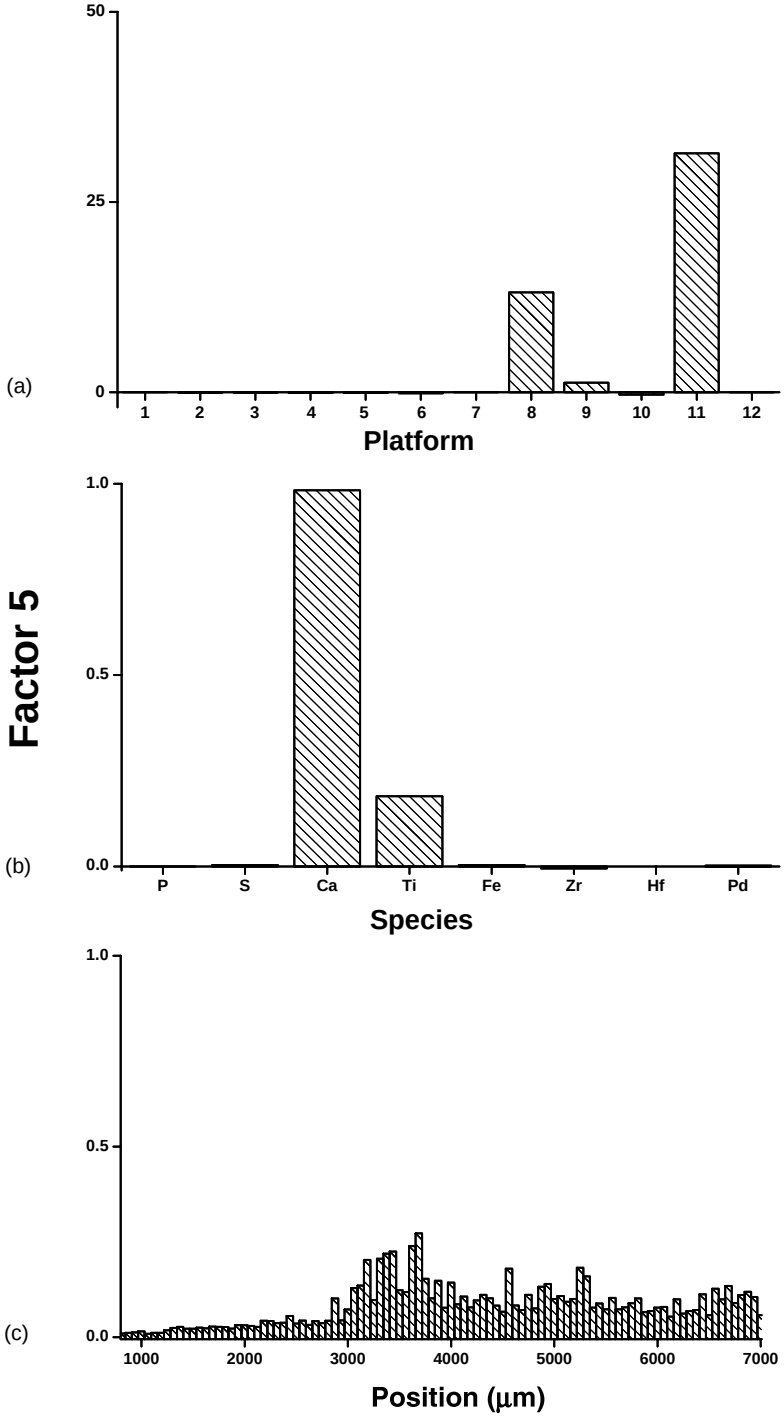

Fig. 6. PARAFAC results for factor 5: (a) platform mode; (b) species mode; and (c) position mode loadings.

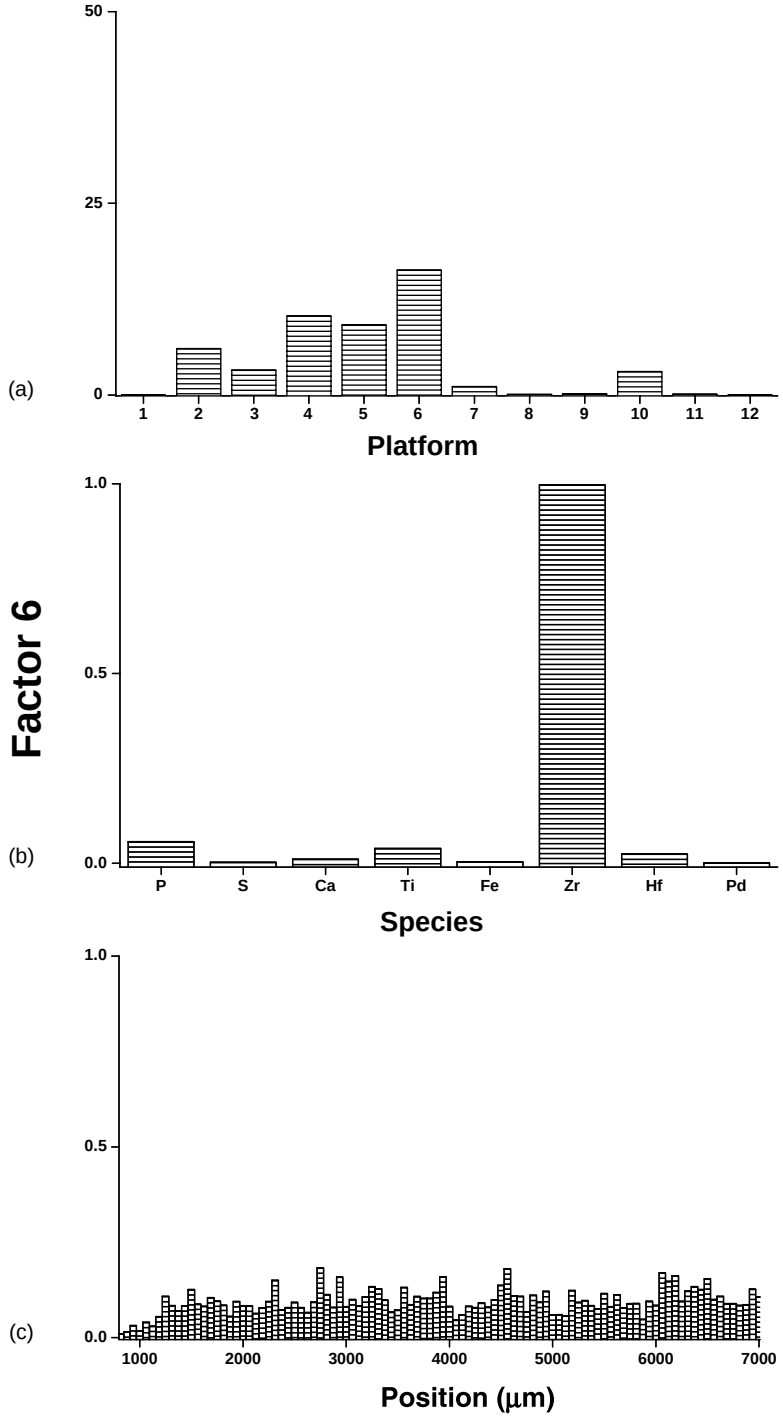

Fig. 7. PARAFAC results for factor 6: (a) platform mode; (b) species mode; and (c) position mode loadings.

for 82.2% of the total variance. A seven-factor model was considered inappropriate because it presented a core consistency of 35.0%. The first four factors of the six-factor constrained model were very similar to the four factors of the previous unconstrained model.

Figs. 2 and 3 show the results found for factors 1 and 2, respectively. These factors were related to the platforms treated with Pd + Mg and used for Pb (platform 12) (Fig. 2) and Cd (platform 9) (Fig. 3) determination, respectively. The platform 12 is mainly characterised by the presence of Pd and Fe (Fig. 2b) in the platform centre (Fig. 2c). On the other hand, the platform 9 has a great S influence (Fig. 3b) on the platform edge (Fig. 3c). Sulphur can be originated from the bovine liver certified samples, which presented a concentration of 7850 $\mu g\, g^{-1}$. The application of PARAFAC modelling showed the differentiation of the preferential places where some phenomena occurred considering Cd or Pb atomisation in the L'vov platform. In the platform treated with Pd + Mg, it seems that the central part of the platform plays a more important role in the Pb determination (Fig. 2c). In addition, when Cd is considered (platform also treated with Pd + Mg), the edges of the L'vov platform are more influenced by the atomised Cd (Fig. 3c). These observations are in agreement with those obtained with image PCA (Fig. 1), which indicate that the central part and edges present morphology different from the rest of the platforms.

Fig. 4 shows the results of PARAFAC factor 3. This factor modelled the platform treated with Zr and used for 500 heating cycles in Al determination (Fig. 4a, platform 7). As it is observed in Fig. 4b, this platform has signals of significant fluorescence intensity produced by Hf and Zr. The most significant positions were at the centre and the right side (Fig. 4c). This information was not observed when applying bi-dimensional PCA.

Figs. 5a and 6a show that platforms treated with Zr and Mg and used for Cd, Pb and Al determinations (platforms 10, 11 and 8, respectively) have a remarkable influence due to a high P and Ca content (Figs. 5b and 6b). For the platform 10, modelled by factor 4, and used for Cd determination, this influence was mainly observed at the left side of the platform (Fig. 5c). The platforms 11 and 8, both modelled by factor 5, presented Ca in all positions (Fig. 6c), but higher fluorescence intensity at the centre of the platform. The presence of a high Ca signal in the platform 8 can be attributed to a not complete platform modification by Mg. This fact probably lead to higher surface degradation, which was showed for platform 8 in

Table 3
Summary of results obtained by PARAFAC

PARAFAC factor number (explained variance (%))	Platform modelled	Species with more influence	Platform region with more influence	Remark
1 (18.6)	12	Fe and Pd	Centre	In spite of the presence of Pd from the conventional modification, this metal was not successful in Fe elimination.
2 (18.0)	9	P, Ca, Pd, Fe, Ti and mainly S	Edges	S, P, Ca and Fe were probably from the slurry sample.
3 (17.8)	7	Hf and Zr	Centre and right side	Platform used for Al determination and 500 heating cycles.
4 (11.4)	10	Ti and mainly P	Left side	P is probably from the bovine liver slurry sample.
5 (11.3)	8 and 11	Ti and mainly Ca	Centre and right side	Mg and Pd + Mg conventional modifiers were not successful in Ca elimination; as previously indicated by image PCA, the centre of platform 8 has a particular behaviour.
6 (5.0)	2–6 and 10	Zr	All	As observed by using image PCA and confirmed by PARAFAC, these platforms presented the same behaviour.

image PCA. This information was also not observed when applying bi-dimensional PCA.

Finally, Fig. 7 shows factor 6. This figure shows the new platform treated with Zr and the platforms also treated with this modifier and used for Al determination for 50, 100, 150 and 200 heating cycles (Fig. 7a). All platforms were separated and mainly characterised by Zr presence (Fig. 7b) in the whole platform extension (Fig. 7c).

Table 3 summarises all the information extracted from the PARAFAC data modelling, including the positions of L'vov platforms that contribute on the phenomena involved in the Al, Cd or Pb determinations. As it can be seen from this table, for those elements presenting lower atomisation temperature (Cd and Pb (platforms numbers 9–12)) the processes involved in the atomisation take place preferentially at the edges for Cd and in the centre for Pb. However, when Al (platforms numbers 2–8) is considered, these processes seem to occur in different positions on the platform surface and depend on the number of heating cycles and on the modifier. For the platforms used for 500 heating cycles (platforms 7 and 8), the main atomisation process occur at the centre and at the right side when the platform is treated with Zr (platform 7) and mainly at the centre when the platform is treated with Mg (platform 8). Conversely, the platforms numbers 2–6 (0, 50, 100, 150 and 200 heating cycles) presented a similar behaviour among them, where the Zr is equally distributed in the whole extension of platforms. In addition, as the atomisation temperature in this case is high (2400 °C), the agitation of the system is increased, thus contributing to the diffusion of the species through the platform. Such kind of diffusion depends on the modifier, for example, Zr was efficient in Ca elimination, but when Mg was used Ca was detected as a concomitant.

5. Conclusion

It is important to point out that the use of image PCA in combination with PARAFAC allowed to extract information according to the morphology and the surface metal interactions at different positions in the L'vov platforms. The PARAFAC modelling of the data obtained by μSRXRF permitted to get a global characterisation of the platforms, summarised in Table 3. Four platforms, 12, 9, 7 and 10, presented a particularly behaviour, being so different among themselves, that it was necessary one specific factor (1–4) to model each one. Factor 5 demonstrated that platforms 8 and 11 presented a similar behaviour characterised by high Ca and, to a lesser extent, Ti content. Finally, factor 6 modelled the correlated behaviour of platforms 2–6 characterised by Zr content.

In addition, with this work it was observed that the platform morphology has a good connection with the residual species found in its surface. A good example is the platform used for Al determination and treated conventionally with Mg. This platform presented Ca distributed in its whole extension, and, mainly at the central part Figs. 1 and 6c). The platforms used for Al determination, treated with Zr and heated for 50, 100, 150 and 200 times presented only Zr in its surface (Fig. 7) and presented a similar behaviour when image PCA was applied (Fig. 1).

As already mentioned in the PARAFAC section (Section 4), an univariate analyses of this data could be performed, but in this case this procedure can lead to visualisation and interpretation problems due to the great amount of data. As an example, S content in platform 9 was only evidenced by using PARAFAC. If the data were analysed in an univariate way, this important information probably could be not detected, because the S signal is too small when compared to the other species present in this platform.

Such kind of studies can open a vast field to exploratory analysis of L'vov platforms in ETAAS. With the results obtained in this work we suppose that the atomisation rate might be different depending on the position and/or pathways, the modifier, the sample and the analyte.

Acknowledgements

The authors are grateful to the Fundação de Amparo a Pesquisa do Estado de São Paulo (FAPESP, São Paulo, Brazil) for a fellowship to ERPF and the financial support (grant numbers 99/00259-5 and 99/12124-7) and to the Conselho Nacional de Desenvolvimento Científico e Tecnológico (CNPq, Brasília, Brazil) for fellowships to MMS, RJP and MAZA.

References

[1] N.J. Miller-Ihli, J. Anal. At. Spectrom. 4 (1989) 295.
[2] W. Frech, D.C. Baxter, B. Hütsch, Anal. Chem. 58 (1986) 1973.
[3] W. Slavm, D.C. Manning, Spectrochim. Acta Part B 37 (1982) 955.
[4] N.J. Miller-Ihli, Spectrochim. Acta Part B 44 (1989) 1221.
[5] F. Barbosa Jr., E.C. Lima, F.J. Krug, Analyst 125 (2000) 2079.
[6] C. Bendicho, M.T.C. Loos-Vollebregt, J. Anal. At. Spectrom. 6 (1991) 353.
[7] E.R. Pereira-Filho, C.A. Pérez, R.J. Poppi, M.A.Z. Arruda, Spectrochim. Acta Part B 57 (2002) 1259.
[8] A.B. Volynsky, Spectrochim. Acta Part B 53 (1998) 139.
[9] Z. Benzo, A. Garaboto, F. Ruette, M. Quintal, V. León, Spectrochim. Acta Part B 52 (1997) 1305.
[10] J.P. Matousek, H.K.J. Powell, Talanta 44 (1997) 1183.
[11] V. Majidi, R.G. Smith, N. Xu, M.W. McMahon, R. Bossio, Spectrochim. Acta Part B 55 (2000) 1787.
[12] E. De Giglio, L. Sabbatini, L. Lampugnani, V.I. Slaveykova, D.L. Tsalev, Surf. Interface Anal. 29 (2000) 747.
[13] K.H.A. Janssens, F.C.V. Adams, A. Rindby, Microscopic X-ray Fluorescence Analysis, Wiley, Chichester, 2000.
[14] H. Martens, T. Naes, Multivariate Calibration, Wiley, New York, 1989, pp. 97–108.
[15] A.K. Smilde, Chemon. Intell. Lab. Syst. 15 (1992) 143.
[16] L. Moberg, G. Robertsson, B. Karlberg, Talanta 54 (2001) 161.
[17] J.C.G.E. da Silva, J.M.M. Leitão, F.S. Costa, J.L.A. Ribeiro, Anal. Chim. Acta 453 (2002) 105.
[18] P. Hindmarch, K. Kavianpour, R.G. Brereton, Analyst 122 (1997) 871.
[19] J. Nilsson, S. de Jong, A.K. Smilde, J. Chemom. 11 (1997) 511.
[20] B.M. Wise, N.B. Gallagher, S.W. Butler, D.D. White, G.G. Barna, J. Chemom. 13 (1999) 379.
[21] R. Leardi, C. Armanino, S. Lanteri, L. Alberotanza, J. Chemom. 14 (2000) 187.
[22] R. Bro, Chemon. Intell. Lab. Syst. 38 (1997) 149.
[23] R. Bro, Multi-way analysis in the food industry, Ph.D. Thesis, Amsterdan, 1998.
[24] P.M. Kroonenberg, Three Mode Principal Component Analysis: Theory and Applications, DSWO, Leiden, 1983.
[25] R. Bro, J. Chemom. 10 (1996) 47.
[26] P. Geladi, H. Grahn, K. Esbensen, E. Bengtsson, Trends Anal. Chem. 11 (1992) 121.
[27] P. Geladi, H. Grahn, Multivariate Image Analysis, Wiley, Chichester, 1996.
[28] L. Munck, L. Norgaard, S.B. Engelsen, R. Bro, C.A. Andersson, Chemon. Intell. Lab. Syst. 44 (1998) 31.
[29] A. Marcos, M. Foulkes, S.J. Hill, J. Anal. At. Spectrom. 16 (2001) 105.
[30] A. Moreda-Piñeiro, A. Marcos, A. Fisher, S.J. Hill, J. Anal. At. Spectrom. 16 (2001) 360.
[31] E.R. Pereira-Filho, R.J. Poppi, M.A.Z. Arruda, Mikrochim. Acta 136 (2001) 55.
[32] C.A. Pérez, M. Radtke, H.J. Sánchez, H. Tolentino, R.T. Neuenshwander, W. Barg, M. Rubio, M.I.S. Bueno, I.M. Raimundo, J.J.R. Rohwedder, X-ray Spectrom. 28 (1999) 320.
[33] H.J. Sánchez, C.A. Pérez, M. Grenón, Nucl. Instrum. Method Phys. Res. B 170 (2000) 211.
[34] The THGA Graphite Furnace: Techniques and Recommended Conditions, Technical Documentation, Realise 1.2, Boderseerwerk Perkin-Elmer GmbH, Uberlingen, Germany, 1995.
[35] C.A. Andersson, R. Bro, Chemon. Intell. Lab. Syst. 52 (2000) 1.
[36] R. Bro, A.K. Smilde, Centering and scaling in component analysis, J. Chemom. 17 (2003) 16.
[37] R. Bro, H.A.L. Kiers, A new efficient method for determining the number of components in PARAFAC models, J. Chemom., in press.
[38] S. Imai, Y. Kubo, A. Yonetani, N. Ogawa, Y. Kikuchi, J. Anal. At. Spectrom. 13 (1998) 1199.
[39] M.C. Almeida, W.R. Seitz, Appl. Spectrosc. 40 (1986) 4.